



City Research Online

City, University of London Institutional Repository

Citation: Reyes-Aldasoro, C. C. ORCID: 0000-0002-9466-2018, Wilson, I., Prise, V., Barber, P., Ameer-Beg, S., Vojnovic, B. and Tozer, G. (2005). Measurement of Vascular Permeability from Multiphoton Microscopy of Experimental Tumours. Poster presented at the NCRI Cancer Conference, 2-5 October 2005, Birmingham, UK.

This is the published version of the paper.

This version of the publication may differ from the final published version.

Permanent repository link: <https://openaccess.city.ac.uk/id/eprint/25613/>

Link to published version:

Copyright: City Research Online aims to make research outputs of City, University of London available to a wider audience. Copyright and Moral Rights remain with the author(s) and/or copyright holders. URLs from City Research Online may be freely distributed and linked to.

Reuse: Copies of full items can be used for personal research or study, educational, or not-for-profit purposes without prior permission or charge. Provided that the authors, title and full bibliographic details are credited, a hyperlink and/or URL is given for the original metadata page and the content is not changed in any way.

Measurement of Vascular Permeability from Multiphoton Microscopy of Experimental Tumours

Constantino Carlos Reyes-Aldasoro¹, Ian Wilson², Vivien Prise², Paul Barber², Simon Ameer-Beg², Borivoj Vojnovic² and Gillian M Tozer^{1,2}

¹ Tumour Microcirculation Group, Surgical Oncology, Royal Hallamshire Hospital, The University of Sheffield
² Gray Cancer Institute, PO Box 100, Mount Vernon Hospital, Northwood, Middlesex HA6 2JR

c.reyes@sheffield.ac.uk



Introduction

An image processing-based algorithm to measure **vascular permeability** of microvessels in 3D tumours is presented. The effect of the tumour vascular targeting drug, **combretastatin A-4-phosphate (CA-4-P)**, on tumour vascular permeability is also analysed. 15 data sets were obtained; 9 treated and 6 controls.

Materials

Animals

P22 rat sarcoma fragments (~ 0.5 mm) were taken from a donor rat, placed into a transparent **window chamber** surgically implanted into the dorsal skinflap of **BD9 male rats** (~ 200 g). Following surgery, animals were given an i.p. injection of 2 ml of dextrose saline and allowed to recover. The tumours were then allowed to establish over a period of 10-14 days to a diameter of 2 to 4 mm. The animals were surgically anaesthetized using a mixture of *fentanyl-fluanisone* and *midazolam* and kept warm on a thermostatically controlled heating blanket.

Multiphoton intravital microscopy

Intravital fluorescent microscopy of **40 kDa FITC-labelled dextran** was performed with a multiphoton microscope system, based on a modified *Bio-Rad MRC 1024MP* workstation, comprising a solid state pumped (10 W Millennia X, Nd:YVO4, Spectra Physics), self mode locked Ti:Sapphire (Tsunami, Spectra Physics) laser system, a focal scan head, confocal detectors and an inverted microscope (Nikon TE200). The leakage of marker was imaged as a time series of 3D tumour volumes (Figure 1).

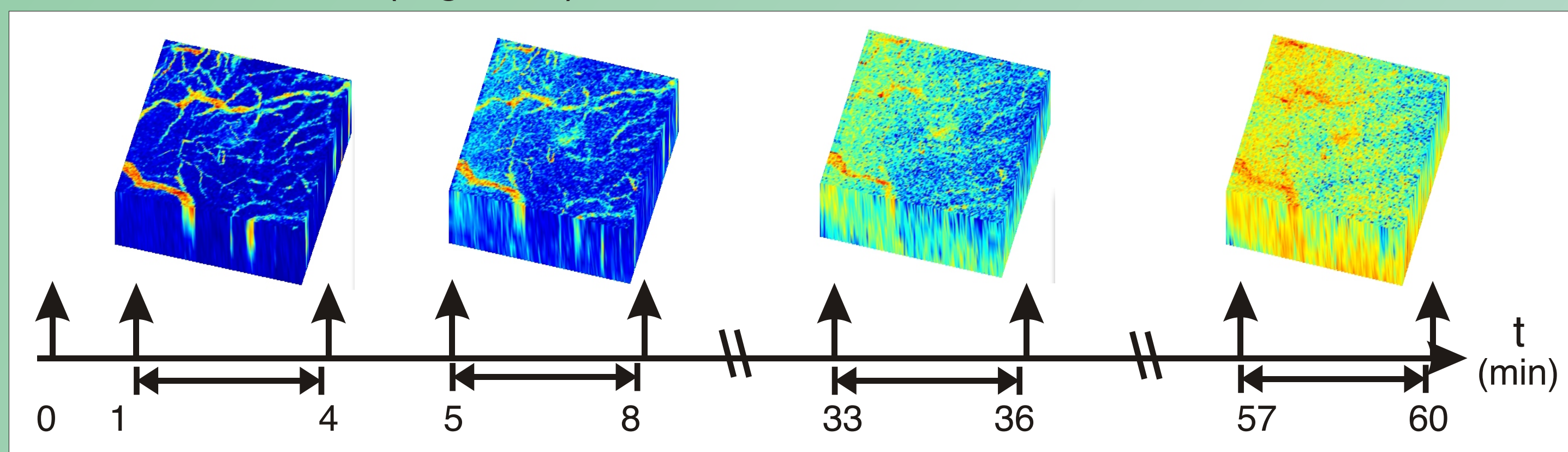


Figure 1 Four time samples (1,2,9,15) of the 3D images to be analysed. Each volume contains 512x512x11 elements and was acquired in a 3 min period. The marker was injected at time $t=0$. The change in colour represents and increase in the intensity of the marker.

Methods

Previous attempts to solve this problem assumed cylindrical vessels and required hand delineation regions of interest, which is both unreliable and time consuming. The following preprocessing steps were required before the measurements were extracted (all the processing was performed in *Matlab*.)

Noise removal

The image acquisition process is noisy and the concentration of the marker varies along the image. Using an *OctTree* it was possible to reduce the noise and the uncertainty in the intensity at the expense of the spatial resolution.

Deformations

As the time samples were acquired, the data suffered from deformations within the window chamber. Figure 2 presents the deformation in a time cut.

Deformations were corrected with rigid registration -- the whole image was shifted towards a certain direction -- or non-rigid registration -- the data was partitioned and registered by regions according to each case. Registration was performed by **cross correlation** in the **Fourier domain**.

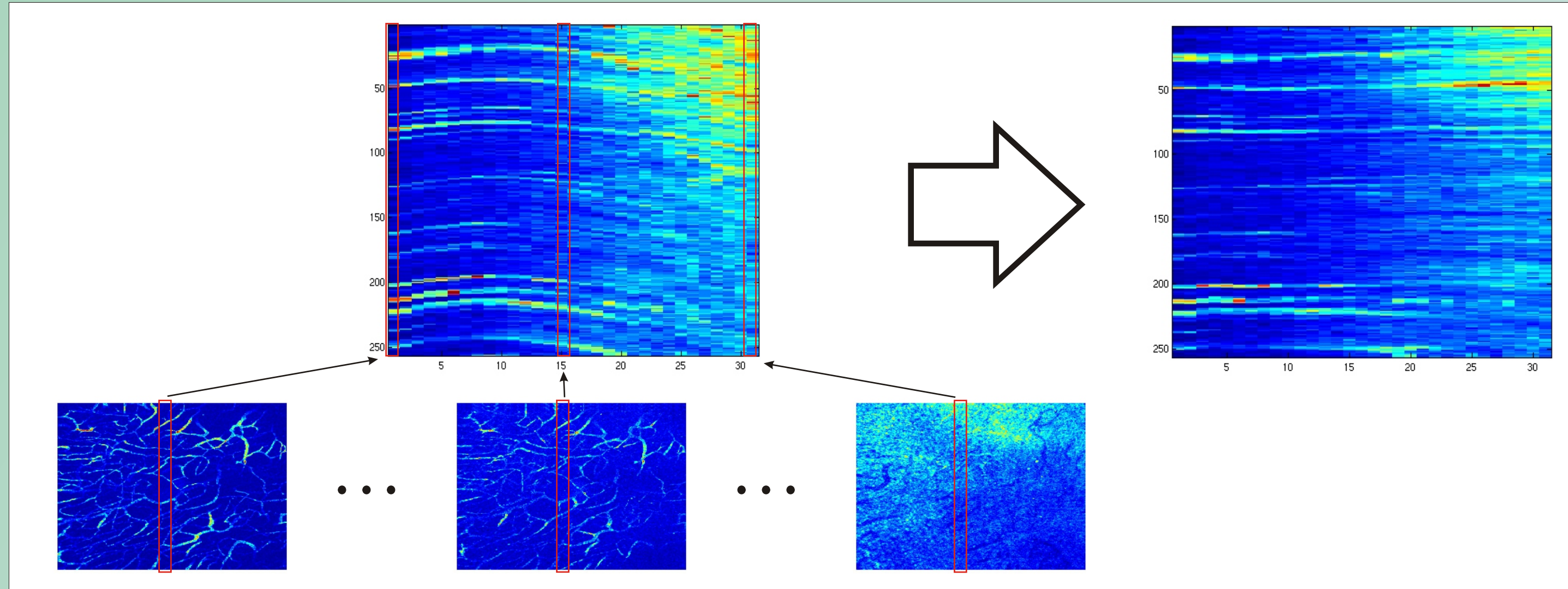


Figure 2 A time cut for one data set. Columns of different time samples are placed next to each other to create a 2D image with time as the x axis. This reveals the deformation, and the corrected set on the right.

Segmentation

A **double threshold** was used to distinguish *vessels*, *tissue* and an *uncertainty* region. A boundary region of the vessels was obtained through a convolution with a Gaussian kernel to approximate the surface. Figure 3 presents the 3D class mask and a rendered volume of the vessels. In the mask brown represents vessels, orange represents tissue and blue and green the surrounding boundaries of the vessels.

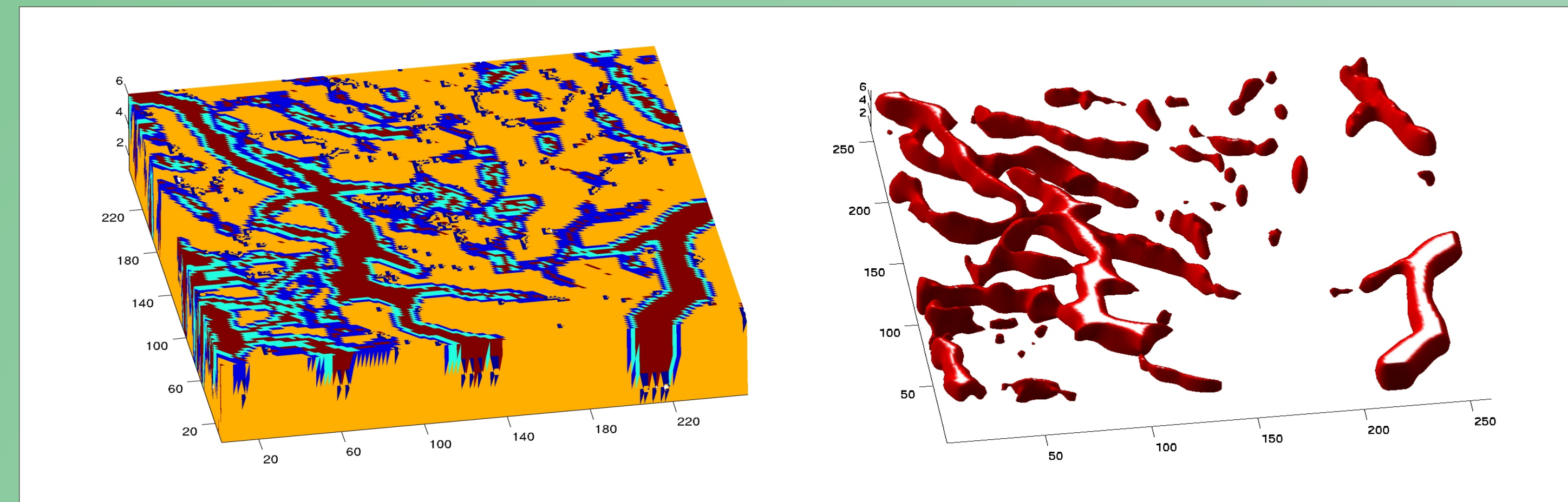


Figure 3 Volumetric class mask and rendering of the segmented vessels.

To verify the accuracy of the segmentation a set was hand segmented and the traces compared with the semiautomatic results, 92.7% of the traces were correct and only 7.3% were incorrect and those ones corresponded to low intensity regions which are hard even for a human expert (Figure 4.)

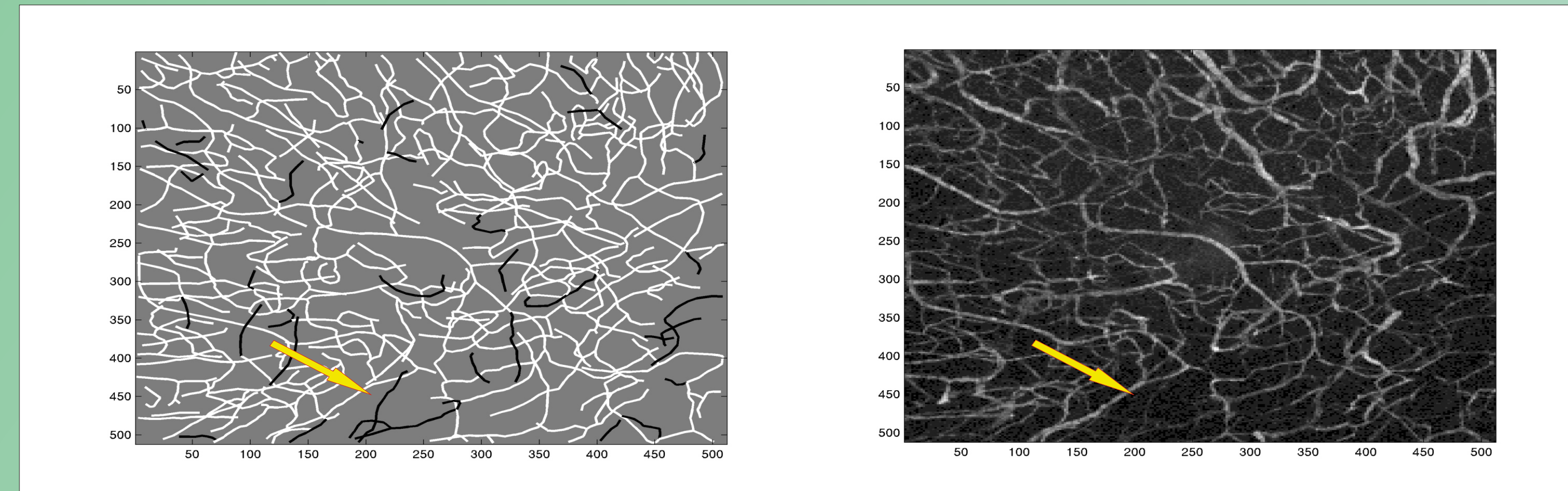


Figure 4 Semiautomatic and manual segmentation comparison. White lines correspond to correct traces and black to incorrect. Notice how incorrect traces belong to low intensity regions.

Results

Intensity in time and Patlak plots

For every time sample t , the concentration on tissue C_t and vessels C_p were calculated as the average intensity of the pixels determined by the segmented mask. Patlak plots [3] model the supply of blood as a system of compartments with uni- and bidirectional flows and linearises the kinetic behaviour of the movement between compartments. Figure 5 shows one intensity and three Patlak plots. The slope of the plots is related to the permeability-surface per volume unit product (PS/V). The permeability was calculated from this value and the estimated surface and volume of the sets. Figure 6 shows the corresponding boxplots.

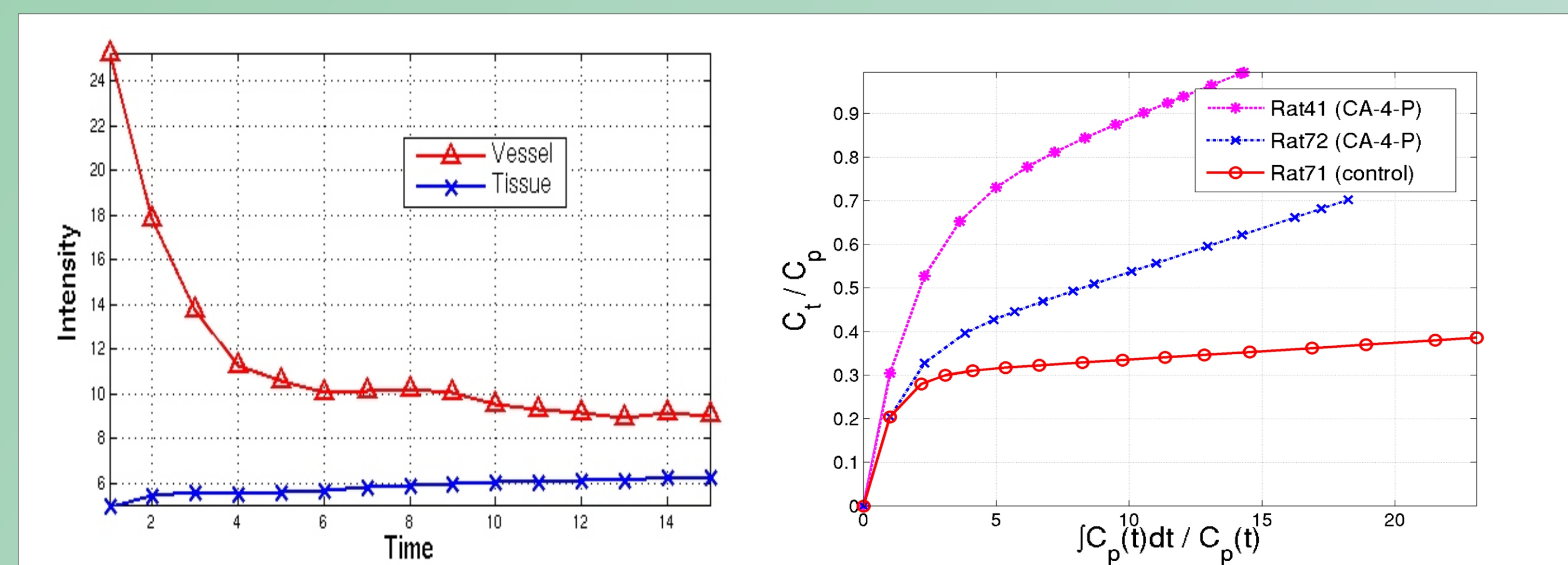


Figure 5 Intensity plot of the tissue and vessel classes, and three Patlak plots. Notice the different slopes of controls and CA-4-P.

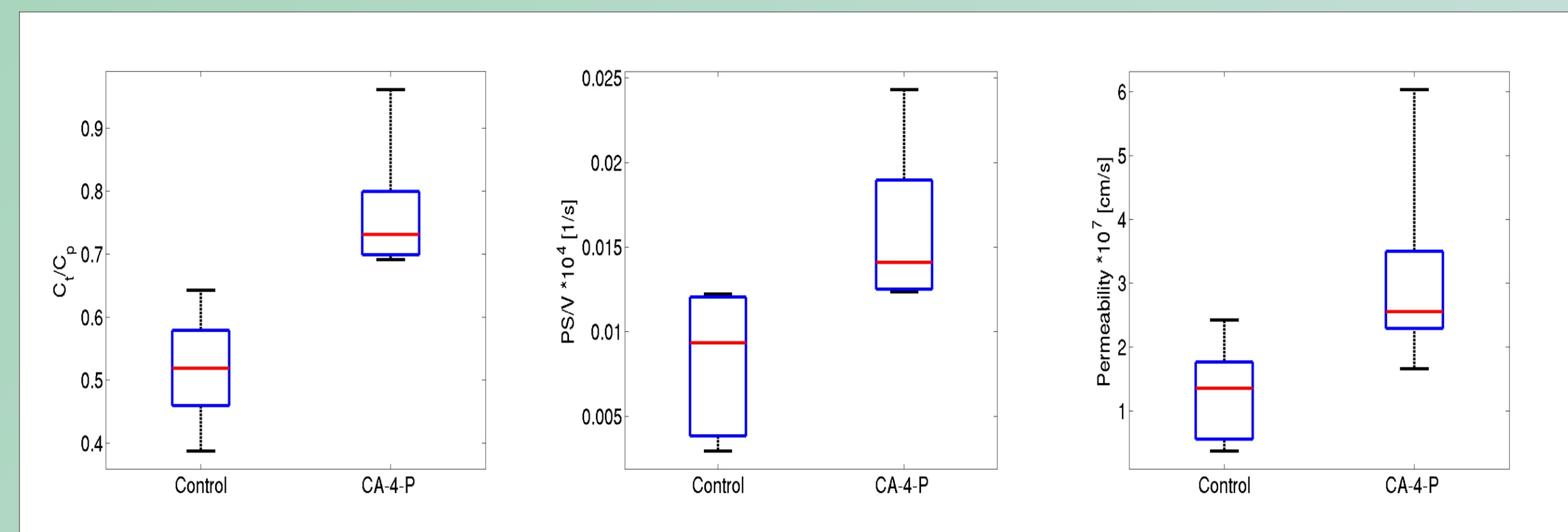


Figure 6 Boxplots of C_t/C_p ($p=0.00016$), PS/V ($p=0.0049$) and permeability ($p=0.021$).

Conclusions

The method presented can measure **vascular permeability** in a **simpler** and **more reliable** way than previously available. Tumours that are treated with CA-4-P manifest **higher permeability** than controls.

References

- [1] Tozer G. M., Prise V. E., Wilson J., Locke R. J., Vojnovic B., Stratford M. R., Dennis M. F., Chaplin D. J. Combretastatin A-4 Phosphate as a tumour vascular targeting agent: early effects in tumours and normal tissues. *Cancer Res.* 59, 1626-34 (1999)
- [2] C. Kanthou and G.M. Tozer. The tumour vascular targeting agent Combretastatin A-4 Phosphate induces reorganization of the actin cytoskeleton and early membrane blebbing in human endothelial cells. *Blood*, 15, 2060-69 (2002)
- [3] Clifford S. Patlak and Ronald G. Blasberg. Graphical evaluation of blood-to-brain transfer constants from multiple-time uptake data. Generalizations. *Journal of cerebral blood flow and metabolism*, 5, 584-590 (1985)